Indian Journal of Radio & Space Physics
Vol. 19, June 1990, pp. 154-165

A one-dimensional model for minor neutral constituents in the mesosphere and lower thermosphere

T S N Somayaji & T Arunamani
Space Physics Laboratories, Andhra University, Visakhapatnam 530 003

Received 4 August 1988; revised received 6 January 1989

A time dependent one-dimensional model for the middle atmospheric minor neutral constituents of aeronomic interest is worked out. The model considers transport only in the vertical direction and calculates the vertical distributions of the minor neutral constituents in the altitude range 60-120 km, at intervals of 2 km, for specified solar and terrestrial conditions. These conditions are specified through (i) the solar radiation fluxes in 120 wavelength bands in the range 116.3-435.0 nm, (ii) the solar zenith angle and vertical distributions of temperature, (iii) eddy diffusion coefficient and (iv) the number densities of O_2 and N_2 in the atmosphere. Model derived results for solar minimum conditions, characterized by a sunspot number of 20 and for a solar zenith angle of 30° at low latitudes, are presented. The results are representative of noontime annual mean values for a latitude of 11°N and are discussed in the light of similar model results and observations reported earlier.

1 Introduction

The minor neutral constituents such as O_3, OH, NO, $O(^3P)$ etc., play an important role in the atmospheric phenomena in the upper atmosphere. In the mesosphere and the lower thermosphere, the minor constituents are important for the ionchemistry and are crucial for the ion composition of that region. There, the variations in the concentrations of atomic oxygen (O) and nitric oxide (NO) cause changes in the electron density distribution. The chemical reactions that determine the neutral composition have longer time constants, when compared to those of the ion-chemical reactions, and therefore the variations in the ionization composition of the D- and E-regions are mainly determined by the variations in the neutral composition.

In the upper atmosphere, the minor constituents of aeronomic interest are mostly produced from the interaction of the solar radiation with the atmosphere. The products of the photochemical reactions are usually chemically highly active and give rise to a variety of chemical reactions in the upper atmosphere. These photochemical and chemical reactions combined with the transport processes that take place there, eventually lead to an equilibrium distribution of the minor constituents. Often this equilibrium distribution of minor constituents which arises from particular solar and terrestrial conditions is of interest.

Variations of the distributions of atmospheric minor constituents, arising from variations in solar and terrestrial conditions, have been of scientific interest for quite some time now. This interest has considerably increased following the observations of Crutzen[1] and Johnston[2] on the destructive influence of NO on the atmospheric ozone. Numerical simulation studies involving mathematical models are used for such studies. The mathematical models must take into account all known physical and chemical processes of the atmosphere and must be able to reproduce all the key measurable parameters accurately. The inputs to such models are usually taken from the observations or, calculated, within the model, in a self consistent way based on more basic principles and fundamental data. The accuracy of a model which is based on inputs taken from observations is, to an extent, determined by the accuracy of the observations that have been used as inputs. The advantage in calculating as many parameters as possible in a self consistent way from more basic principles is, therefore, obvious.

Of the various minor neutral constituents of the middle atmosphere, NO has a large source in the thermosphere. The global average production of NO above 100 km is about two orders of magnitude larger than the NO source strength in the stratosphere, as was pointed out by Crutzen[1]. The NO has relatively longer chemical lifetime in the thermosphere and, therefore, can survive transport to lower altitudes. Thus NO distribution in the mesosphere can be influenced by NO in the thermosphere. For this reason, it is necessary to include the

contribution of NO from the thermosphere in middle atmospheric models. We have, therefore, worked out the model for the altitude range 60-120 km, although our main interest, for the present, is the mesosphere.

In this paper we have worked out a one-dimensional model for the mesospheric minor constituents of aeronomic interest and discussed the results obtained from it in the light of similar model results and observations reported earlier.

2 Chemical reactions and data

The chemical reactions that have been considered for the model are shown in Table 1. The reaction rate coefficients that have been adopted for this study are based on JPL publication No. 82-57 (Ref. 3).

The oxygen species $O(^3P)$, $O(^1D)$, O_3 and $O_2(^1\Delta_g)$ are produced mainly by the photodissociation of O_2 into atomic oxygen and the subsequent reactions involving the atomic oxygen. The odd hydrogen species H, OH and HO_2 are produced by the photodissociation of water vapour and the subsequent reactions involving the photodissociation products. The odd nitrogen species N, NO and NO_2 have different sources at different altitudes. At the mesospheric heights, NO, the key species of the odd nitrogen group, is mainly produced by the photodissociation of N_2 and the subsequent oxidation of atomic nitrogen. At higher altitudes, in the thermosphere, NO is produced from reactions involving atomic nitrogen. Some of the atomic nitrogen in the thermosphere come from the reactions involving the ionized species. The atomic nitrogen produced in these reactions can be either in the ground state [$N(^4S)$] or, in an excited state, primarily [$N(^2D)$]. Finally, NO is formed by the reaction of the atomic nitrogen with O_2. The mutual destruction of odd nitrogen occurs through the reactions involving atomic nitrogen [$N(^4S)$, $N(^2D)$] with NO, in which N_2 and O are produced. Of these reactions, the one involving $N(^4S)$ is much slower than the one involving $N(^2D)$. Therefore, the probability of destruction of NO through N is greater for $N(^4S)$ than for $N(^2D)$. This implies that the odd nitrogen distribution is influenced by the branching ratios of production of $N(^4S)$ and $N(^2D)$ in reactions involving the ionized species. Higher the ratio of the $N(^2D)$ production relative to $N(^4S)$ production is, higher will be the odd nitrogen concentrations. From laboratory measurements, Kley *et al.*[4] have found that 75% of the atomic nitrogen produced in the dissociative recombination of NO^+ is in the ^2D level. Ogawa and Shimazaki[5] and Kondo and Ogawa[6] have adopted a value of 90% for this. In the present work we have assumed the following relative production rates for $N(^2D)$ and $N(^4S)$ in the reactions involving ionization species.

$NO^+ + e \rightarrow N + O$	[$N(^2D)$-87%; $N(^4S)$-13%]
$N_2^+ + e \rightarrow 2N$	[$N(^2D)$-50%; $N(^4S)$-50%]
$N_2^+ + O \rightarrow NO^+ + N$	[$N(^2D)$-50%; $N(^4S)$-50%]

The ionization reactions that are considered for accounting the thermospheric production of NO, are taken from Banks and Kockarts[7] and are given in Tabel 2. The reaction rate constants that have been adopted for these reactions are also given in Table 2. The necessary ionization frequencies of N_2, O_2, O and NO are based on the compilation by Deshpande *et al.*[8]

For calculating the production of NO through reactions involving the ionized species, one needs to know an electron density distribution. In the present study an electron density distribution based on observations is assumed. This is given by:

$$N_e = 10^{(z-50)/10}; \quad z < 100 \text{ km} \qquad \ldots (1)$$

$$N_e = 1.0 \times 10^5; \quad 100 < z < 120 \text{ km} \qquad \ldots (2)$$

The solar radiation in the spectral interval 116.3-435.0 nm is considered responsible for the dissociation of different air molecules. The data for the solar flux and the absorption cross-sections of the various air molecules in this spectral interval are taken from the compilation by Deshpande and Mitra[9].

Sasi and Sengupta[10] have constructed a reference atmosphere for the Indian equatorial zone for the altitude range 0-80 km. This reference atmosphere is adopted for the temperature and air density data needed for the present model calculations. Above 80 km, appropriate data from CIRA-1972 (Ref. 11) are taken and suitably adjusted for matching the data at the boundary, viz. 80 km. The densities of N_2 and O_2 are obtained from the mean air density assuming constant mixing ratios of 78.083% and 20.947% for N_2 and O_2, respectively.

3 Photodissociation

The photodissociation coefficients for all compounds, except NO, are calculated as usual from

$$J(X) = \int_\lambda I_\lambda^\infty . \sigma_\lambda(X) . \exp(-\tau) . d\lambda \qquad \ldots (3)$$

$$\tau(\chi, z) = \left[\sigma_\lambda(O_2) . \int_z^\infty n(O_2)\, dz + \sigma_\lambda(O_3) . \int_z^\infty n(O_3)\, dz \right] . \sec\chi \qquad \ldots (4)$$

Table 1—Reactions of neutral species used in the model

Reaction number	Reaction	Rate constant $cm^n s^{-1}$	Wavelength nm
R_{1a}	$O_2 + h\nu \rightarrow O(^1D) + O(^3P)$		$\lambda < 175$
R_{1b}	$O_2 + h\nu \rightarrow O(^3P) + O(^3P)$		$175 < \lambda < 240$
R_{2a}	$O_3 + h\nu \rightarrow O_2(^1\Delta_g) + O(^1D)$		$\lambda < 310$
R_{2b}	$O_3 + h\nu \rightarrow O_2 + O(^3P)$		$\lambda > 310$
R_3	$O + O + M \rightarrow O_2(^1\Delta_g) + M$	$3(-33) \times (T/300)^{-2.9}$	
R_4	$O + O_3 \rightarrow O_2 + O_2(^1\Delta_g)$	$1.5(-11) \times \exp(-2297/T)$	
R_5	$O + O_2 + M \rightarrow O_3 + M$	$6.25(-34)(T/300)^{-2.45}$	
R_{6a}	$O(^1D) + O_2 \rightarrow O + O_2$	$5.5(-11)$	
R_{6b}	$O(^1D) + N_2 \rightarrow O + N_2$	$5.0(-11)$	
R_{6c}	$O(^1D) + O_2 \rightarrow O + O_2(^1\Delta_g)$	$1.0(-12)$	
R_7	$O + OH \rightarrow H + O_2$	$4.0(-11)$	
R_8	$O_3 + OH \rightarrow HO_2 + O_2$	$1.6(-12) \times \exp(-940/T)$	
R_9	$H + O_3 \rightarrow OH + O_2$	$1.4(-10) \times \exp(-470/T)$	
R_{10}	$H + O_2 + M \rightarrow HO_2 + M$	$2.1(-32) \times \exp(290/T)$	
R_{11}	$HO_2 + O \rightarrow OH + O_2$	$4.0(-11)$	
R_{12}	$HO_2 + O_3 \rightarrow OH + 2O_2$	$1.4(-14) \times \exp(-580/T)$	
R_{13}	$HO_2 + NO \rightarrow OH + NO_2$	$3.4(-12) \times \exp(250/T)$	
R_{14}	$H + OH + M \rightarrow H_2O + M$	$2.5(-31)$	
R_{15}	$HO_2 + HO_2 \rightarrow H_2O_2 + O_2$	$3.9(-14) \times \exp(1245/T)$	
R_{16}	$H_2O + O(^1D) \rightarrow OH + OH$	$2.3(-10)$	
R_{17}	$H_2O + h\nu \rightarrow H + OH$		$\lambda < 190$
R_{18}	$H + OH \rightarrow H_2 + O$	$1.0(-12) \times T^{1/2} \times \exp(-4000/T)$	
R_{19a}	$H + HO_2 \rightarrow H_2 + O_2$	$0.29 \times 4.7(-11)$	
R_{19b}	$H + HO_2 \rightarrow H_2O + O$	$0.02 \times 4.7(-11)$	
R_{19c}	$H + HO_2 \rightarrow OH + OH$	$0.69 \times 4.7(-11)$	
R_{20}	$H + H + M \rightarrow H_2 + M$	$1.2(-32) \times (273/T)^{0.7}$	
R_{21}	$HO_2 + OH \rightarrow H_2O + O_2$	$4.0(-11)$	
R_{22}	$OH + OH \rightarrow H_2O + O$	$1.0(-11) \times \exp(-500/T)$	
R_{23}	$N + O_2(^1\Delta_g) \rightarrow NO + O$	$3.0(-15)$	
R_{24}	$N + NO_2 \rightarrow O + N_2O$	$1.75(-12) \times T^{1/2}$	
R_{25}	$N + O_3 \rightarrow NO + O_2$	$5.0(-12)$	
R_{26}	$N + O_2 \rightarrow NO + O$	$5.0(-13) \times T^{1/2} \times \exp(-3500/T)$	
R_{27}	$N + OH \rightarrow NO + H$	$5.0(-11)$	
R_{28}	$N + O + M \rightarrow NO + M$	$1.0(-32) \times (300/T)^{1/2}$	
R_{29}	$NO + O_3 \rightarrow NO_2 + O_2$	$2.3(-12) \times \exp(-1450/T)$	
R_{30}	$NO_2 + O \rightarrow NO + O_2$	$9.3(-12)$	
R_{31}	$NO_2 + h\nu \rightarrow NO + O$		$\lambda < 400$
R_{32}	$NO + h\nu \rightarrow N + O$		$\lambda < 191$
R_{33}	$N + NO \rightarrow N_2 + O$	$3.4(-11)$	
R_{34}	$N(^2D) + O_2 \rightarrow NO + O$	$5.0(-11)$	
R_{35}	$N_2O + O(^1D) \rightarrow NO + NO$	$5.9(-11)$	
R_{36}	$NO + O + M \rightarrow NO_2 + M$	$6.0(-32) \times (300/T)^{3/2}$	
R_{37}	$NO + NO + O_2 \rightarrow NO_2 + NO_2$	$1.0(-33)$	
R_{38}	$NO + O \rightarrow NO_2 + h\nu$	$6.4(-17)$	
R_{39}	$N_2 + h\nu \rightarrow N + N$	Ref. 7	
R_{40}	$O_2(^1\Delta_g) + O_2 \rightarrow O_2 + O_2$	$2.17(-18) \times (T/300)$	
R_{41}	$O_2(^1\Delta_g) \rightarrow O_2 + h\nu_{1.27\,\mu m}$	$2.8(-4)$	

Note: Read $a(m)$ as $a \times 10^m$, e.g. $4.0(-11) = 4.0 \times 10^{-11}$; $n = 3$ for binary reactions and $n = 6$ for three body reactions.

Table 2—Reactions of ion species used in the model

Reaction number	Reaction	Rate constant $cm^3\ s^{-1}$
I_{N_2}	$N_2 + h\nu \rightarrow N_2^+ + e$	Ref. 8
α_{N_2}	$N_2^+ + e \rightarrow N(^2D) + N(^2D)$	$F_{N_2} \times 3(-7) \times (300/T)^{0.33}$
	$N_2^+ + e \rightarrow N(^4S) + N(^4S)$	$(1 - F_{N_2}) \times 3.0(-7) \times (300/T)^{0.33}$
γ_3	$N_2^+ + O \rightarrow NO^+ + N(^2D)$	$F_O \times 1.4(-10)$
	$N_2^+ + O \rightarrow NO^+ + N(^4S)$	$(1 - F_O) \times 1.4(-10)$
γ_9	$N_2^+ + O_2 \rightarrow N_2 + O_2^+$	$4.7(-11) \times (300/T)$
I_{O_2}	$O_2 + h\nu \rightarrow O_2^+ + e$	Ref. 8
α_{O_2}	$O_2^+ + e \rightarrow O + O$	$2.2(-7) \times (300/T)$
γ_5	$O_2^+ + NO \rightarrow O_2 + NO^+$	$6.3(-10)$
γ_6	$O_2^+ + N \rightarrow O + NO^+$	$1.8(-10)$
γ_7	$O_2^+ + N_2 \rightarrow NO + NO^+$	$2.0(-16)$
I_O	$O + h\nu \rightarrow O^+ + e$	Ref. 8
γ_1	$O^+ + N_2 \rightarrow NO^+ + N(^4S)$	$1.0(-12) \times (300/T)$
γ_2	$O^+ + O_2 \rightarrow O + O_2^+$	$2.2(-11) \times (300/T)$
γ_{4a}	$O^+ + NO \rightarrow O + NO^+$	$1.3(-12)$
γ_{4b}	$O^+ + NO \rightarrow N(^4S) + O_2^+$	$1.0(-12)$
I_{NO}	$NO + h\nu \rightarrow NO^+ + e$	Ref. 8
α_{NO}	$NO^+ + e \rightarrow N(^2D) + O$	$F_{NO} \times 4.1(-7) \times (300/T)^{1.5}$
	$NO^+ + e \rightarrow N(^4S) + O$	$(1 - F_{NO}) \times 4.1(-7) \times (300/T)^{1.5}$

Note: Read $a(m)$ as $a \times 10^m$, e.g. $1.0(-12) = 1.0 \times 10^{-12}$

where, I_λ^∞ is the solar flux incident at the top of the atmosphere, τ the optical depth factor of the radiation in the wavelength interval λ and $\lambda + d\lambda$, and $\sigma_\lambda(X)$ is the absorption cross-section of the species X at wavelength λ.

For evaluating τ, it is assumed that the absorbers of radiation in the wavelength interval of interest are O_2 and O_3 only. For computing τ, a distribution of O_3 which is consistent with direct observations is assumed. This is of the form

$$n(O_3) = 10^{(16-z/10)} \qquad \ldots (5)$$

The evaluation of the photodissociation coefficient for NO is more involved because of the overlap of NO absorption bands and S – R bands of O_2. The transmission of radiation through the S – R band interval of O_2 was discussed by Cieslik and Nicolet[12] and suitable parametrizations were suggested by Nicolet and Peetermans[13] and Allen and Frederick[14]. The photodissociation coefficient of NO can be calculated from one of these parametrizations. In the present work, however, the photodissociation rates for NO are adopted from the work of Solomon[15]. The altitude profiles of photodissociation coefficients of the various species are shown in Fig. 1.

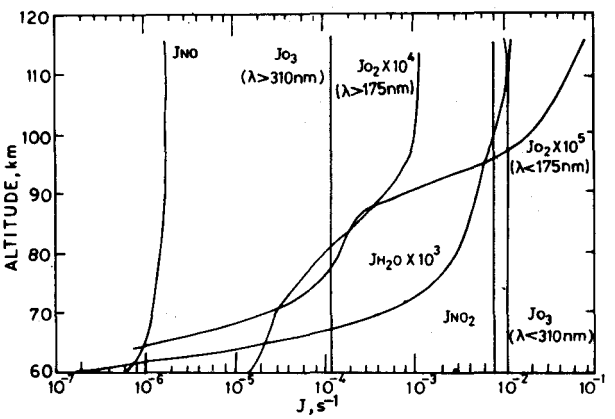

Fig. 1—Altitude profiles of photodissociation coefficients of various species

4 Transport

The model considers transport only in the vertical direction. The transport formulation adopted for the present work is as follows

$$\nabla.\phi \approx \partial\phi/\partial z; \quad \phi = \phi_m + \phi_e \qquad \ldots (6)$$

$$\phi_m = -D_m\{[\partial n(X)/\partial z] + [(1+\alpha)n(X)/T] \times (\partial T/\partial z) + n(X)/H_x\} \qquad \ldots (7)$$

$$\phi_e = -K.n(M).\partial\mu(X)/\partial z \qquad \ldots (8)$$

$$= -[\{K_{i-1}n(M)_{i-1} + K_i.n(M)_i\} \times \{\mu(X)_i - \mu(X)_{i-1}\}]/(2.\Delta z) \qquad \ldots (9)$$

$$\partial\phi/\partial z = (\phi_{i+1} - \phi_i)/\Delta z \qquad \ldots (10)$$

where

ϕ	Total vertical flux of any constituent
ϕ_m, ϕ_e	Vertical flux due to molecular and eddy diffusion, respectively
D_m	Mutual diffusion coefficient between the constituent gas and molecular nitrogen
K	Vertical eddy diffusion coefficient
$\mu(X)$	Volume mixing ratio of the constituent gas, X, given by $\mu(X) = n(X)/n(M)$
$n(X)$	Number density of the constituent gas
$n(M)$	Mean air density (number density)
T	Atmospheric temperature
α	Thermal diffusion factor
H_x	Scale height of the constituent X
Δz	Altitude interval

The suffix 'i' indicates the altitude at which the calculations are made.

For the present work, the eddy diffusion coefficient distribution is taken from the work of Holton[16] and is shown in Fig. 2. Fig. 2 also shows a K profile based on the work of Ebel[17]. This is used for studying the effect of variations in K on the model derived distributions of atomic oxygen and NO as discussed in Sec. 8.

A value of 0.17 is adopted for the thermal diffusion factor, α. Calculations are made at height intervals of 2 km in the altitude range 60-120 km.

5 Computation technique

The calculations of the distribution of odd oxygen [$O(^3P)$, $O(^1D)$ and O_3], odd hydrogen (H, OH and HO_2) and odd nitrogen (N, NO and NO_2) species are made in two steps. First, the distributions are calculated assuming photostationary conditions and adopting the H_2O profile derived by Solomon[15]. Secondly, the distributions of the various species are determined by obtaining the time dependent solutions of the respective continuity equations.

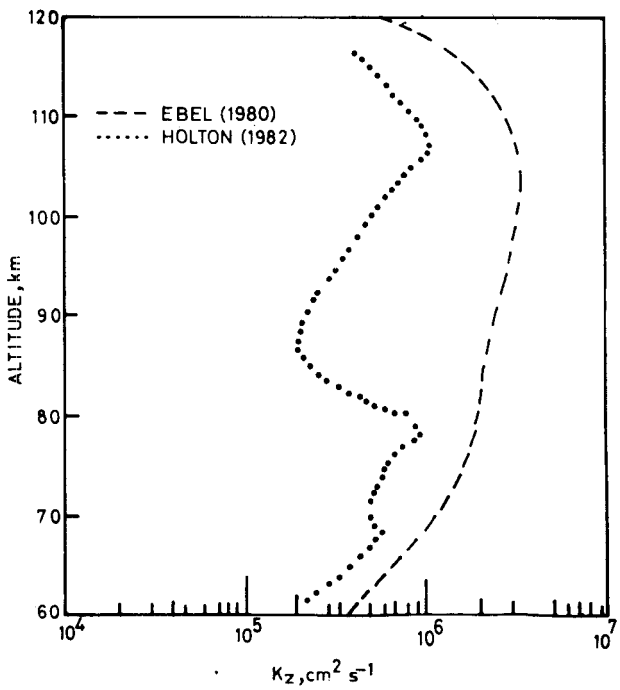

Fig. 2—Profiles of vertical eddy diffusion coefficients

Considering only the dominant terms in the continuity equations for different species and assuming equilibrium conditions, one can obtain the equations for the concentrations of different species as follows.

$$n[O(^3P)] = \{[(R_{1a} + R_{1b}).(R_{2a} + R_{2b}).n(O_2) - \{R_{10}.n(O_2).n(M) + R_9.n(O_3)\}.n(H)]/[R_3.(R_{2a} + R_{2b}) + R_5.R_4.n(O_2) \times n(M)]\}^{1/2} \quad \ldots (11)$$

$$n[O(^1D)] = [R_{1a}.n(O_2) + R_5.n\{O(^3P)\} \times n(O_2).n(M)]/[R_{6b}.n(N_2) + (R_{6a} + R_{6c}).n(O_2)] \quad \ldots (12)$$

$$n(O_3) = R_5.n(O).n(O_2).n(M)/[R_{2a} + R_{2b} + R_9.n(H)] \quad \ldots (13)$$

$$n(H) = \{R_{17}.n(H_2O)/[C.(R_{19a} + R_{21}.D)]\}^{1/2} \quad \ldots (14)$$

$$n(HO_2) = R_{10}.n(O_2).n(M).n(H)/[R_{11}.n(O)] \quad \ldots (15)$$

$$n(OH) = [R_{11}.n(HO_2).n(O) + R_9.n(O_3).n(H)]/[R_7.n(O)] \quad \ldots (16)$$

where

$n(O) = n\{O(^3P)\} + n\{O(^1D)\}$

$C = R_{10}.n(O_2).n(M)/[R_{11}.n(O)]$

$D = [R_{10}.n(O_2).n(M) + R_9.n(O_3)]/[R_7.n(O)]$

First, the distributions of the odd oxygen species in a pure oxygen atmosphere (i.e., neglecting the effect of the hydrogen species) are determined from Eqs (11)-(13). Using these distributions, the distributions of odd oxygen and odd hydrogen species in an oxygen-hydrogen atmosphere are determined iteratively from Eqs (11)-(16), till convergence to within one per cent deviation is obtained. Finally, the distribution of $O_2(^1\Delta_g)$ is calculated assuming photostationary conditions between O_3 and $O_2(^1\Delta_g)$ as follows.

$$n[O_2(^1\Delta_g)] = R_{2a}.n(O_3)/[R_{40}.n(O_2) + R_{41}] \quad \ldots (17)$$

For the equilibrium concentrations of the odd nitrogen species, one can obtain the following equations.

$$A.n^2(NO) + B.n(NO) + C_1 = 0 \quad \ldots (18)$$

where

$$A = 2R_{33}.[R_{32} + \gamma_{4b}.n(O^+) + (1-F_{NO}).\{I_{NO} + \gamma_{4a}.n(O^+)\} + (1-F_{NO}).\gamma_5.n(O_2^+)]$$

$$B = R_{33}.[2R_{39}.n(N_2) + 2n(N_2).W.I_{N_2}.(1-F_{N_2}) + 2.Y.I_O.(1-F_{NO}) - \gamma_7.n(O_2^+).n(N_2).F_{NO} + \gamma_3.2n(O).n(N_2^+).(2F_{N_2} - F_{NO} - F_O)]$$

$$C_1 = -[bn + \gamma_6.F_{NO}.n(O_2^+)] \times [\gamma_7.n(O_2^+).n(N_2).(2+F_{NO}) + 2n(N_2).(R_{39} + W.I_{N_2}) + 2Y.I_O.F_{NO}.n(O)]$$

$$W = [\alpha_{N_2}.N_e + \gamma_3.n(O)]/[\alpha_{N_2}.N_e + \gamma_3.n(O) + \gamma_9.n(O_2)]$$

$$Y = \gamma_1.n(N_2)/[\gamma_1.n(N_2) + \gamma_2.n(O_2)]$$

$$bn = R_{28}.n(O).n(M) + R_{26}.n(O_2) + R_{23}.n[O_2(^1\Delta_g)] + R_{25}.n(O_3) + R_{27}.n(OH)$$

$$n(N) = \{n(NO).[R_{32} + \gamma_{4b}.n(O^+) + (1-F_{NO}).(I_{NO} + \gamma_{4a}.n(O^+)) + (1-F_{NO}).\gamma_5.n(O_2^+)] + 2n(N_2).[R_{39} + W.I_{N_2}.(1-F_{N_2}) + Y.I_O.n(O).(2-F_{NO})] + \gamma_3.n(O).n(N_2^+).(2F_{N_2} - F_{NO} - F_O) + \gamma_7.n(N_2).n(O_2^+)\}/[bn + \gamma_6.F_{NO}.n(O_2^+) + R_{33}.n(NO)] \quad \ldots (19)$$

$$n(NO_2) = n(NO).[R_{36}.n(O).n(M) + R_{29}.n(O_3) + R_{13}.n(HO_2) + R_{38}.n(O)]/[R_{30}.n(O) + R_{31}] \quad \ldots (20)$$

Here I represents the ionization frequency of the molecule indicated by the suffix.

The distributions of N, NO and NO_2 are determined using Eqs (18)-(20) in which the terms F_{NO}, F_O and F_{N_2} correspond to the fraction of production of atomic nitrogen in the ^2D state in reactions involving the ionized species as indicated in Table 2 and mentioned in Sec. 2.

The distribution of the various species, determined as above, are used as initial values for the second step of calculations. In second step, the distributions are determined by obtaining time-dependent solutions of the respective continuity equations. To save computational time, the various species are grouped into families. The odd oxygen and odd hydrogen species are separately grouped into two families. The species NO and NO_2 are grouped together and treated as one family. Atomic nitrogen is treated independently.

Omitting less important terms, the continuity equation for the odd oxygen (O_x) family and its partition into its member species can be written as follows.

$$dn(O_x)/dt = 2R_1.n(O_2) - \{R_8.n(OH).[n(O_3)/n(O_x)] + R_{12}.n(HO_2).[n(O_3)/n(O_x)] + R_9.n(H).[n(O_3)/n(O_x)] + 2R_4.n(O_3).[n(O)/n(O_x)] + R_7.n(OH).[n(O)/n(O_x)] + R_{11}.n(HO_2).[n(O)/n(O_x)] + 2R_3.n(O).n(M).[n(O)/n(O_x)]\} \times n(O_x) - \partial\phi(O_x)/\partial z \quad \ldots (21)$$

Assuming steady state for ozone, the ratio of ozone to atomic oxygen can be written as

$$n(O_3)/n(O) = R_5.n(O_2).n(M)/[R_{2a} + R_{2b} + R_9.n(H)] = A_{o_x} \text{ (say)} \quad \ldots (22)$$

Neglecting $n[O(^1D)]$ in comparison with $n[O(^3P)]$, one gets

$$n(O)/n(O_x) = 1/(1+A_{o_x}); \text{ and } n(O_3)/n(O_x) = A_{o_x}/(1+A_{o_x}) \quad \ldots (23)$$

Similarly for odd hydrogen

$$dn(HO_x)/dt = 2R_{17}.n(H_2O) + 2R_{16}.n[O(^1D)] \times n(H_2O) - \{2R_{21}.[n(OH)/n(HO_x)] \times [n(HO_2)/n(HO_x)] + 2.(R_{19a} + R_{19b}).[n(H)/n(HO_x)] \times [n(HO_2)/n(HO_x)] + 2R_{15}.[n(HO_2)/n(HO_x)] \times [n(HO_2)/n(HO_x)] + 2R_{14}.n(M).[n(OH)/n(HO_x)] \times [n(H)/n(HO_x)] + 2R_{18}.[n(OH)/n(HO_x)] \times [n(H)/n(HO_x)] + 2R_{20}.n(M) \times [n(H)/n(HO_x)].[n(H)/n(HO_x)] + 2R_{22}.[n(OH)/n(HO_x)].[n(OH)/n(HO_x)]\}.n(HO_x).n(HO_x) - \partial\phi(HO_x)/\partial z \quad \ldots (24)$$

$$n(H)/n(OH) = R_7.n(O)/[R_9.n(O_3) + R_{10}.n(O_2).n(M)] = A_{h_x} \quad \ldots (25)$$

$$n(HO_2)/n(OH) = [A_{h_x}.R_{10}.n(O_2).n(M) + R_8.n(O_3)]/[R_{11}.n(O) + R_{13}.n(NO)] = B_{h_x} \quad \ldots (26)$$

$$n(OH)/n(HO_x) = 1/[1 + A_{h_x} + B_{h_x}] \quad \ldots (27)$$

$$n(HO_2)/n(HO_x) = [n(OH)/n(HO_x)].B_{h_x} \quad \ldots (28)$$

$$n(H)/n(HO_x) = [n(OH)/n(HO_x)].A_{h_x} \quad \ldots (29)$$

For the odd nitrogen species ($NO_x = NO + NO_2$), the relevant equations are:

$$dn(NO_x)/dt = bn.n(N) + R_{34}.n[N(^2D)].n(O_2) + \gamma_7.n(O_2^+).n(N_2) - [R_{32} + I_{NO} + (\gamma_{4a} + \gamma_{4b}).n(O^+) + \gamma_5.n(O_2^+) + R_{33}.n(N)].[n(NO)/n(NO_x)] \times n(NO_x) - \partial\phi(NO_x)/\partial z \quad \ldots (30)$$

The term bn appearing in Eq. (30) was already defined in Eq. (18). The ratio, $n(NO_2)/n(NO)$, required to partition the odd nitrogen into its member species, can be obtained from Eq. (20). If this ratio is denoted by A_{n_x}, the concentrations of NO and NO_2 can be written in terms of NO_x as:

$$n(NO) = n(NO_x)/[1 + A_{n_x}] \quad \text{and}$$

$$n(NO_2) = [A_{n_x}.n(NO_x)]/[1 + A_{n_x}] \quad \ldots (31)$$

Similarly for the atomic nitrogen species, we have

$$dn[N(^4S)]/dt = n(N_2).[2R_{39} + \gamma_1.n(O^+).(2 - F_{NO}) + \gamma_7.n(O_2^+)] + 2.(1 - F_{N_2}) \times \alpha_{N_2}.n(N_2^+).N_e + n(NO) \times \{R_{32} + (1 - F_{NO}).I_{NO} + n(O^+).[(1 - F_{NO}).\gamma_{4a} + \gamma_{4b}] + (1 - F_{NO}).\gamma_5.n(O_2^+)\} + \gamma_3.n(N_2^+).n(O).(2F_{N_2} - F_{NO} - F_O) - [R_{33}.n(NO) + bn + F_{NO} \times \gamma_6.n(O_2^+)].n(N) - \partial\phi(N)/\partial z \quad \ldots (32)$$

$$dn[N(^2D)]/dt = F_{NO}.\{\alpha_{NO}.n(NO^+).N_e\} + 2F_{N_2}.\alpha_{N_2}.n(N_2^+).N_e + F_O.\gamma_3.n(N_2^+).n(O) - R_{34}.n(O_2).n[N(^2D)] \quad \ldots (33)$$

where

$$\alpha_{NO}.n(NO^+).N_e = n(NO).[I_{NO} + \gamma_{4a}.n(O^+) + \gamma_5.n(O_2^+)] + \gamma_1.n(O^+) \times n(N_2) + \gamma_3.n(N_2^+).n(O) + \gamma_6.n(N).n(O_2^+) + \gamma_7.n(N_2).n(O_2^+) \quad \ldots (34)$$

Time-dependent solutions of the above differential equations are obtained to determine the concentrations of the families at time $t + \Delta t$ as follows.

The continuity equation for any species X has the general form

$$dn(X)/dt = P_t - L_{t+\Delta t}.(X)_{t+\Delta t} - \partial\phi(X)_t/\partial z \ldots (35)$$

where, P and L are, respectively, the total production and loss rate of the species 'X' from all the chemical processes. The suffix t indicates the time at which the different terms are evaluated.

The term $n(X)_{t+\Delta t}$ is obtained by writing Eq. (35) in its implicit difference form as follows.

$$\frac{n(X)_{t+\Delta t} - n(X)_t}{t} = P_t - L_{t+\Delta t}.n(X)_{t+\Delta t} - \partial\phi(X)_t/\partial z \quad \ldots (36)$$

Assuming $L_{t+\Delta t} \approx L_t$, and by suitable transformation, Eq. (36) can be written as

$$n(X)_{t+\Delta t} = \{[P_t - \partial\phi(X)_t/\partial z].\Delta t + n(X)_t\}/[1 + L_t.\Delta t] \quad \ldots (37)$$

Assuming the distributions of the various species calculated in step one as the initial distributions for $n(X)$ at time t, corresponding to the chosen solar zenith angle, the differential fluxes in the vertical direction $[\partial\phi(X)_t/\partial z]$, the chemical production (P_t) and the loss rate (L_t) are calculated at different altitudes. Appropriate boundary conditions at the lower and upper boundaries are prescribed by defining $\phi(X)$ or $n(X)$ to calculate the differential fluxes across the lowest and highest altitudes. Using these values in Eq. (36), the concentrations of the species 'X', i.e. $n(X)_{t+\Delta t}$, at the next time step Δt are calculated for different altitudes starting from the highest altitude and working downwards. Using the distributions obtained at time $t + \Delta t$, as the initial values, the calculations are repeated to obtain yet another set of distributions appropriate for time $t + 2\Delta t$. This calculation procedure is repeated until distributions for a time $t + 24$ hr, are obtained. Then the distributions calculated for time $t + 24$ hr and time t are compared for agreement or otherwise. In case the disagreement in the concentrations of any species at any altitude is more than a prescribed limit, the calculations are repeated after replacing the initial set assumed for time t with those derived for time $t + 24$ hr. The calculations are continued till convergence to within the prescribed limits of error is achieved. The calculations are repeated for a further period of 24 hr and the distributions at different times are noted down.

In these calculations, the photolysis rates are held fixed for daytime at their values appropriate for the chosen solar zenith angle, and brought to zero between sunset and sunrise. The photolysis rates are updated after every ten days of integration.

6 Choice of time step and grouping of species into families

The time step for integration must be so chosen that it is smaller than any of the characteristic times of the species 'X' for transport and chemical loss. For computational economy, this time step must be as large as possible. If a number of chemical species, which are in chemical equilibrium among themselves, are grouped together and considered as a single family of species, the chemical lifetime of such a family will be much larger than the chemical lifetimes of the member species of the family. Therefore, by suitably grouping the species into families, significant computational speed, and hence economy, can be achieved through the use of a larger time step for integration.

Based on the ideas mentioned above, the different species are grouped into families. The odd oxygen species [$O(^3P)$, $O(^1D)$ and O_3] are considered together as a single entity of odd oxygen family (O_x). Similarly, the odd hydrogen species (H, OH and HO_2) are together considered as the odd hydrogen family (HO_x) and $NO + NO_2$ is considered as the odd nitrogen family (NO_x). The atomic nitrogen is treated independently.

Time dependent solutions were obtained simultaneously for the continuity equations written separately for each of the families at altitude steps of 2 km. The concentrations of individual member species of the families are derived from the family concentrations assuming fixed ratios between member species under chemical equilibrium. During time periods, when the chemical lifetimes of species are not small enough to justify grouping into a family, the family approach is discarded and each species of the family is treated independently.

As a result of the grouping of species into families, it has been found that a time step of 1200 s could be used for integration and the same is adopted for the present study. However, at sunset the time step is reduced to 200 s, for a period of 2 hr of integration, so as to allow for smooth transition of components that rapidly vary with photolysis rates.

7 Boundary conditions

The model calculates the minor constituents distributions in the altitude range 60-120 km. To evaluate the vertical differential fluxes at the different altitudes in the altitude range of interest, which appear in the set of continuity equations, one needs to consider fluxes across the boundaries of different layers. These fluxes across the boundaries of all altitude steps, except the lowest and highest ones, can be calculated from the distributions of the constituent species. The fluxes across the lower and upper boundaries need to be prescribed in the form of either fluxes or as number densities based on observations or physically justifiable considerations.

The odd oxygen species are produced mainly by the interaction of solar UV radiation with molecular oxygen. Atomic oxygen is the dominant member of the odd oxygen family. The odd oxygen species, after being produced in the thermosphere, move downwards. The downward flux at the upper boundary can, therefore, be taken as twice the column rate of photodissociation of molecular oxygen above the upper boundary as pointed out by Thomas and Bowman[18]. Therefore, the downward flux of odd oxygen at 120 km is prescribed as

$$\phi(O_x) = 2.J(O_2).H(O_2) \qquad \ldots (38)$$

where $J(O_2)$ and $H(O_2)$ are the photolysis rate and scale height of O_2 at 120 km, respectively, and $\phi(O_x)$ is the downward flux of the odd oxygen at 120 km.

The odd hydrogen species are produced from H_2, H_2O and CH_4 in the stratosphere and mesosphere through oxidation and photodissociation processes. In the mesosphere and lower thermosphere, atomic hydrogen is the dominant member of this family. The atomic hydrogen concentrations at 100 km, deduced from the measurements of the absorption of the solar lyman-α line by geocoronal atomic hydrogen, are of the order of 10^7 cm^{-3} and less than 2.7×10^7 cm^{-3} as pointed out by many workers[19-21]. Based on these values, a number density of 1.0×10^7 cm^{-3} at 120 km is chosen for odd hydrogen which is also consistent with the atomic hydrogen flux at 120 km derived by Liu and Donahue[22].

The dominant species of the odd nitrogen family is NO. The estimation of the downward flux of NO at 120 km is complex, because it involves the ion-chemistry of the E- and F-regions. Since no estimate of NO_x flux value at 120 km is available, we have prescribed a number density of 6.7×10^7 cm^{-3} for NO_x at 120 km based on a 2-D model calculation by Solomon[15] for a latitude of 11°N and equinoctial conditions.

Based on the 2-D model calculations by Solomon[15], we have prescribed the following concentrations at the lower boundary (60 km) in our calculations.

$n(O_x) = 0.11 \times 10^{11}$ cm^{-3}

$n(HO_x) = 0.11 \times 10^{8}$ cm^{-3}

$n(NO_x) = 0.10 \times 10^{9}$ cm^{-3}

8 Model results and some comparisons

Model calculations are made for typical solar minimum conditions, characterized by $R_z = 20$, and for a solar zenith angle of 30°. The results are believed to be representative annual mean values for a noontime at a low latitude (11°N). Because the photolysis rates are held constant through the day and are brought to zero during night (Sec. 6), the model results are to be interpreted as representative average values for the chosen solar zenith angle. However, the distributions obtained for midday and midnight periods may be used for discerning day-night changes, if any.

The results for odd oxygen species are shown in Fig. 3 which shows the model results of atomic oxygen [O(^{3}P)] obtained by Solomon[15] from similar model calculations for equinox at a latitude of 30°N. Measured values of ozone concentrations reported earlier are also shown for comparison.

Above 70 km most of the odd oxygen is in the form of atomic oxygen [O(^{3}P)] in its ground state. Because of the difficulty in the measurement of this species at mesospheric heights, few measurements of atomic oxygen are available for comparison. Dickinson *et al.*[23] reported daytime vertical concentrations of atomic oxygen at midlatitudes derived from simultaneous rocket measurements of resonance fluorescence and absorption of 130 nm radiation. Their measurements showed number densities of the order of 10^{10} cm^{-3} between 80 and 90 km, followed by a near-exponential decrease to 10^{11} cm^{-3} at 120 km. Howlett *et al.*[24] using rocket measurements of resonant scattered 130 nm radiation, obtained atomic oxygen distribution at White Sands, New Mexico (33°N), at two hours after local sunset. Their measurements showed that the atomic oxygen distribution has similar features as were found by Dickinson *et al.*[23] An additional feature found by them[24] was a vertical structure with two peaks, one at around 90 km where the number density was 10^{11} cm^{-3} and the other at around 98 km where the number density was 1.2×10^{11} cm^{-3}. They[24] suggested that the double peak structure can be explained on the basis of wind shears.

The vertical distribution of atomic oxygen obtained in the present work exhibits similar features as were reported by Dickinson *et al.*[23] except for a minimum at about 74 km. The steep gradient in the present model derived distribution is located between 83 and 93 km, while a similar gradient was found by Dickinson *et al.*[23] at a little lower height

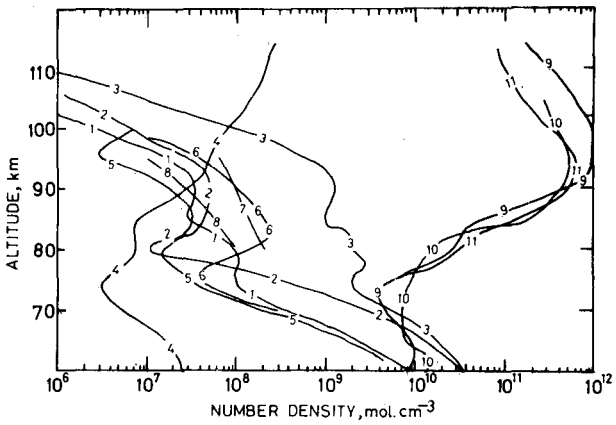

Fig. 3—Altitude distribution of odd oxygen compounds in the mesosphere

[Curve No.	Species	Work
1	O_3 (Day)	Present
2	O_3 (Night)	-do-
3	$O_2(^1\Delta_g)$	-do-
4	$O(^1D) \times 10^3$	-do-
5	O_3	Llewellyn and Witt[26]
6	O_3	Hays and Roble[27]
7	O_3 (Night)	Noxon[38]
8	O_3 (Day)	-do-
9	O(^{3}P)	Present, K_z from Holton[16]
10	O(^{3}P)	Solomon[15]
11	O(^{3}P)	Present, K_z from Ebel[17]]

between 80 and 90 km. The number densities obtained in the present work are in good agreement, particularly above 75 km, with those reported by Dickinson *et al.*[23], but are higher than those obtained by Howlett *et al.*[24] Wasser and Donahue[25] inferred a latitudinal variation of vertical transport of odd oxygen. The differences between the results of our present work and those reported by Howlett *et al.*[24] may have their origin in the differences in the adopted vertical transport.

To examine the effect of vertical transport on the model derived vertical distribution of atomic oxygen, we have calculated the distribution of atomic oxygen adopting a different vertical profile for the eddy diffusion coefficient. The new eddy diffusion coefficient profile was based on the work of Ebel[17] (Fig. 2) and is adopted for the present work. The distribution obtained using Ebel's K profile is also shown in Fig. 3 and is labelled as curve 11. The significant effect of the adopted K values on the model derived results of atomic oxygen concentrations, particularly at altitudes above 75 km, is clearly demonstrated. The vertical distribution obtained by Solomon[15], using a similar model calculation, but for the K profile of Ebel[17], is also shown in Fig. 3 for comparison. The general agreement between our

results and those obtained by Solomon[15] can be noticed.

Llewellyn and Witt[26] have deduced ozone concentrations from rocketsonde measurements of $O_2(^1\Delta_g)$ emission at 1.27 μm. These measurements relate to daytime, but for high latitudes. The agreement between our model deduced ozone concentrations for daytime are in good agreement with those reported by Llewellyn and Witt[26] (Fig. 3). At higher altitudes our model results are higher. The model results show a secondary maximum below 80 km. The results of Llewellyn and Witt[26] show this maximum at around 85 km. We point out that the location of this maximum is dependent on the vertical eddy diffusion and can be moved up and down by changing K.

Hays and Roble[27] derived nighttime vertical distribution of ozone at low latitudes from satellite measurements of intensity of stars in the Hartley continuum during the occultation of stars by the earth's atmosphere. The results reported by these workers are also shown in Fig. 3 for comparison. Their results showed a bulge in the ozone density at around 85 km with a peak of about 2×10^8 cm^{-3}, and a depletion below that altitude. The model deduced results showed a bulge in the ozone density between 80 and 90 km during night. The peak value is 5.4×10^7 mol.cm^{-3} at 88 km. This bulge in the nighttime ozone concentrations was predicted by the theoretical studies carried out earlier by many workers[28-36] following the discussion of Bates and Nicolet[37] on the effect of hydrogen compounds on the atmospheric ozone.

The ozone distributions derived by Noxon[38] from measurements of twilight enhancements of $O_2(b^1\Sigma_g)$ airglow emissions do not show any bulge around 85 km. The model derived ozone profiles for daytime are in reasonable agreement with these earlier results of Noxon[38] and there are considerable differences in the nighttime profiles.

The model derived results for the excited atomic oxygen [O(^{1}D)] and excited molecular oxygen [$O_2(^1\Delta_g)$] are also shown in Fig. 3.

In the mesosphere, odd hydrogen is produced mainly by the photodissociation of water vapour (into H and OH) by the far UV radiation. The perhydroxyl radical (HO_2) is formed by the reactions of atomic hydrogen with O_2 and O_3, and is lost through its reaction with atomic oxygen. The hydroxyl radical is formed by the reaction of HO_2 with O, and is lost through oxidation by atomic oxygen to produce H. It will be clear that the abundances of atomic hydrogen must increase and those of HO_2 and OH must decrease with increase of atomic oxygen. The model derived profiles of the odd hydrogen species, viz. H, OH and HO_2 are shown in Fig. 4. It can be seen that the model derived profile of atomic hydrogen has a peak around 90 km, which is consistent with the above mentioned chemistry and the model derived profile of atomic oxygen which has a peak at about 93 km.

The atomic hydrogen has a long time constant with respect to transport by diffusion when compared to chemical losses, particularly at the higher altitudes. For this reason, like the atomic oxygen, the atomic hydrogen also shows a peak. The model results do reflect this feature and the model calculated profile of atomic hydrogen has a peak at 88 km with the number density 8.4×10^8 cm^{-3}. Above the peak, the profile resembles one arising from diffusive equilibrium, and the abundance of atomic hydrogen decreases nearly exponentially above 88 km. The distribution of atomic hydrogen deduced by Solomon[15] is also shown in Fig. 4 for comparison. Our model results show much larger concentrations, particularly around the peak, although the general features of the two profiles are in agreement.

The OH and HO_2 show a rapid decrease above 75 km as can be seen from the results shown in Fig. 4. This feature can be attributed to the photochemistry. Anderson[39], using resonance fluorescence emissions at 306.4 nm, derived OH profiles up to 70 km. One of these profiles obtained at White Sands, New Mexico is also shown in Fig. 4. Our model results for OH are in good agreement with the measurements of Anderson[39]. The model re-

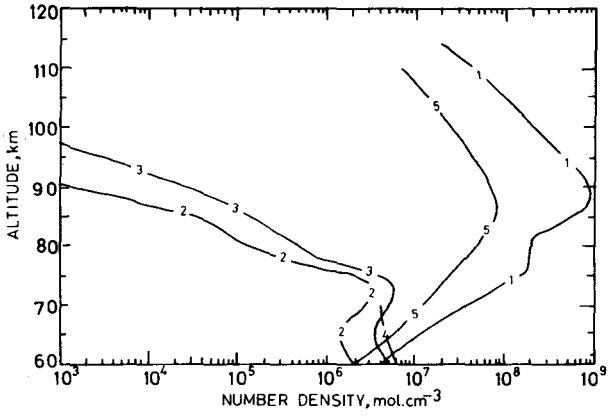

Fig. 4—Altitude distribution of odd hydrogen compounds in the mesosphere

[Curve No.	Species	Work
1	Atomic hydrogen	Present
2	HO_2	-do-
3	OH	-do-
4	OH (measured)	Anderson[39]
5	Atomic hydrogen	Solomon[15]]

sults are also consistent with the measurements made by Anderson[40] and Heaps and McGee[41]. They followed the same method, but used a laser in place of the lamp used earlier by Anderson[39].

The measurements available for HO_2 are sparse and are limited to lower altitudes and, therefore, no comparison of the model derived HO_2 profiles with observations was attempted. However, we wish to point out that the ratio of HO_2 to OH is of the order of unity, which is consistent with the expectations from the photochemical theory.

The odd nitrogen compounds have comparable chemical and diffusive lifetimes in the height range 60-80 km. Above 80 km, the diffusive processes play a relatively more important role in determining the concentrations of NO_x species. The NO_x has a large rate of production above 100 km and, therefore, the prescribed upper boundary conditions and diffusion strongly influence the model calculated NO_x distribution.

The model calculated distributions of odd nitrogen species are shown in Fig. 5. The atomic nitrogen in the excited state (^2D level) is present, in any significant quantity, only above 100 km. The NO which is the dominant odd nitrogen species in the entire altitude range has a minimum of 1×10^7 cm^{-3} at 80 km. The profiles of NO derived from rocket-borne measurements of nitric oxide γ-band emissions in the day airglow by Meira[42] at midlatitudes at a solar zenith angle of 63°, by Tohmatsu and Iwagami[43] and Torkar *et al.*[44] at Thumba, are also shown in Fig. 5 for comparison. The last two measurements[43,44] were made in the same season of the year and nearly at the same local time (solar zenith angle ~ 80°). But the solar activity conditions were very much different. The measurements by Tohmatsu and Iwagami[43] were made under solar minimum conditions ($R_z = 42$) and those by Torkar *et al.*[44] under higher solar activity conditions ($R_z = 118$). Our model results correspond to solar minimum conditions and, therefore, have to be compared with those obtained by Tohmatsu and Iwagami[43]. The agreement is only satisfactory but not very good. Nevertheless, our model results for NO seem to be consistent with those observations.

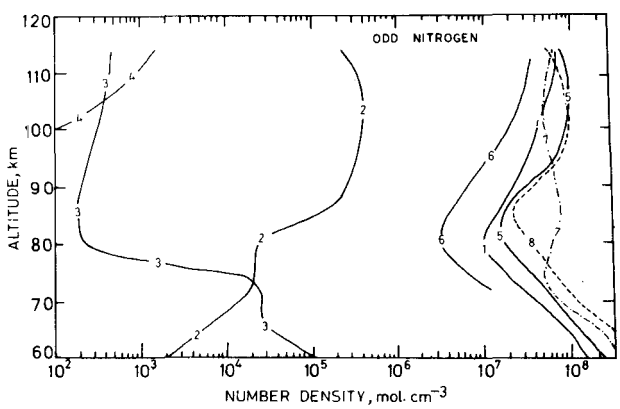

Fig. 5—Altitude distribution of odd nitrogen compounds in the mesosphere

[Curve No.	Species	Work
1	NO	Present, K_z from Holton[16]
2	N(^{4}S).	Present
3	NO_2	-do-
4	N(^{2}D)	-do-
5	NO	Meira[42]
6	NO	Tohmatsu and Iwagami[43]
7	NO	Present, K_z from Ebel[17]
8	NO	Torkar *et al.*[44]]

The NO is a relatively long lived species and the model derived concentrations of NO are expected to be influenced by the choice of eddy diffusion coefficient (K). To examine this aspect, we have also plotted the NO distribution obtained from model calculations which considered a different K distribution (taken from Ebel[17]). This is shown as curve 7 of Fig. 5. The large differences between the two model derived distributions (one using Holton's[16] K profile and the other using Ebel's[17] K profile) show that the NO distributions are sensitively dependent on the eddy diffusion coefficient.

The atomic nitrogen [N(^{4}S)] sharply increases from about 2×10^4 at. cm^{-3} at 80 km to about 3×10^5 at. cm^{-3} at 85 km and thereafter increases slowly with altitude to a maximum of 6×10^5 at. cm^{-3} at 105 km. Above 105 km, the concentration of this species slowly decreases with increasing altitude.

Acknowledgement

This work was carried out under a UGC (IMAP) research project and the authors are thankful to the University Grants Commission, New Delhi, for the financial assistance. The authors had the benefit of useful discussion with their colleagues, Prof. K V V Ramana and Dr D N Madhusudhana Rao, and the same is acknowledged.

References

1 Crutzen P J, *Q J R Meteorl Soc (GB)*, 96 (1970) 320.

2 Johnston H S, *Science (USA)*, 173 (1971) 517.

3 *Chemical Kinetics and Photochemical data for Use in Stratospheric Modelling, J P L Publication* 82-57, *Evaluation No.* 5, USA, 1982.

4 Kley D, Lawrence G M & Stone E J, *J Chem Phys (USA)*, 66 (1977) 4157.

5 Ogawa T & Shimazaki T, *J Geophys Res (USA)*, 80 (1975) 3945.

6 Kondo Y & Ogawa T, *J Geomagn & Geoelectr (Japan)*, 29 (1977) 65.

7 Banks P M & Kockarts G, *Aeronomy* (Academic Press, New York, USA), 1973.

8 Deshpande S D, Jain V C & Mitra A P, *Sci Rep, ISRO-IMAP-SR*-21-85, Bangalore, India, 1985.

9 Deshpande S D & Mitra A P, *Sci Rep, ISRO-IMAP-SR*-11-83, Bangalore, India. 1983.

10 Sasi M N & Sengupta K, *Sci Rep, SPL : SR* : 006 : 85, Vikram Sarabhai Space Centre, Trivandrum, India, 1986.

11 CIRA 1972, *Cospar International Reference Atmosphere* (Academie Verlag, Berlin, GDR), 1972.

12 Cieslik S & Nicolet M, *Planet & Space Sci (GB)*, 21 (1973) 925.

13 Nicolet M & Peetermans W, *Planet & Space Sci (GB)*, 28 (1980) 85.

14 Allen M & Frederick J E, *J Atmos Sci (USA)*, 39 (1982) 2066.

15 Solomon S, *One- and Two-dimensional Photochemical Modelling of the Chemical Interactions in the Middle Atmosphere* 0-120 *km*, Co-operative thesis No. 62, University of California and National Centre for Atmospheric Research, USA, 1981.

16 Holton J R, *J Atmos Sci (USA)*, 39 (1982) 791.

17 Ebel A, *J Atmos & Terr Phys (GB)*, 42 (1980) 617.

18 Thomas L & Bowman M R, *J Atmos & Terr Phys (GB)*, 34 (1972) 1843.

19 Meier R R & Prinz D K, *J Geophys Res (USA)*, 75 (1970) 6969.

20 Meier R R & Mange P, *Planet & Space Sci (GB)*, 18 (1970) 803.

21 Vidal-Madjar A, Blamont J E & Phissamay B, *J Geophys Res (USA)*, 78 (1973) 1115.

22 Liu S C & Donahue T M, *J Atmos Sci (USA)*, 31 (1974) 1118.

23 Dickinson P H G, Bain W C, Thomas L, Williams E R, Jenkins D B & Twiddy N D, *Proc R Soc London Ser A (GB)*, 369 (1980) 379.

24 Howlett C C, Baker K D, Megill L R, Shaw A W, Pendleton W R & Ulwick J C, *J Geophys Res (USA)*, 85 (1980) 1291.

25 Wasser B & Donahue T M, *J Geophys Res (USA)*, 84 (1979) 1297.

26 Llewellyn E J & Witt G, *Planet & Space Sci (GB)*, 25 (1977) 165.

27 Hays P B & Roble R G, *Planet & Space Sci (GB)*, 21 (1973) 273.

28 Hampson J, *Photochemical Behaviour of the Ozone layer, TN* 1627/64, Canadian Armament Research and Development Establishment, Canada, 1964.

29 Hunt B G, *J Atmos Sci (USA)*, 23 (1966) 88.

30 Hunt B G, *J Geophys Res (USA)*, 71 (1966) 1385.

31 Hesstvedt E, *Geophys Norv (Norway)*, 27 (1968) 1.

32 Leovy C B, *J Geophys Res (USA)*, 74 (1969) 417.

33 Bowman M R, Thomas L & Geisler J E, *J Atmos & Terr Phys (GB)*, 32 (1970) 1661.

34 Hunt B G, *J Atmos & Terr Phys (GB)*, 33 (1971) 1869.

35 Shimazaki T & Laird A R, *J Geophys Res (USA)*, 77 (1972) 276.

36 Strobel D F, *Radio Sci (USA)*, 7 (1972) 1.

37 Bates D R & Nicolet M, *J Geophys Res (USA)*, 55 (1950) 301.

38 Noxon J F, *J Geophys Res (USA)*, 80 (1975) 1370.

39 Anderson J G, *J Geophys Res (USA)*, 76 (1971) 7820.

40 Anderson J G, *Geophys Res Lett (USA)*, 3 (1976), 165.

41 Heaps W S & McGee T J, *J Geophys Res (USA)*, 90 (1985) 7913.

42 Meira C G (Jr.), *J Geophys Res (USA)*, 76 (1971) 202.

43 Tohmatsu T & Iwagami N, *J Geomagn & Geoelectr (Japan)*, 28 (1976) 343.

44 Torkar K M, Beran D, Friedrich M & Lal S, *Planet & Space Sci (GB)*, 33 (1985) 1169.